Nanoparticle-block copolymer self-assembly

Scott C. Warren
Department of Chemistry & Chemical Biology
Department of Materials Science & Engineering
Cornell University

Introduction

Fuel cells are a promising technology with respect to power generation because of the potential for efficient conversion of chemical energy to electrical energy. Despite extensive research on proton exchange membrane (PEM) fuel cells, the materials comprising the electrodes are disordered (Fig. 1A), which impedes optimization of structural parameters. A radical improvement in performance, stability, and platinum utilization may be achieved through self-assembly of the electrode (Fig. 1B).

Nanoparticle-block copolymer self-assembly provides a route to design ordered mesostructures (structures with characteristic length-scales of 2 to 50 nm). I discuss the chemistries and design concepts needed to self-assemble ordered mesoporous materials with high metal loadings. First, I present experimental evidence that nanoparticle size dramatically influences self-assembly. Next, I discuss a sol-gel chemistry that incorporates high loadings of metals into electrically conductive mesostructures. I highlight metal nanoparticles with liquid-like behavior that enable the self-assembly of ordered mesoporous metals (Fig. 1B).

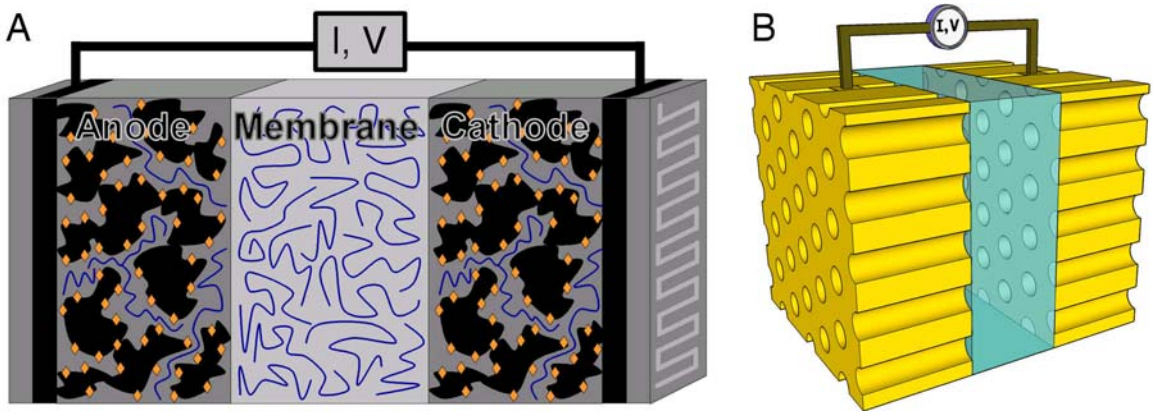

Fig. 1. (A) Diagram of a typical fuel cell, showing the disordered structure of the electrodes. Carbon particles are black, catalyst particles are orange, and polymer is blue. **(B)** Idealized sketch of a fuel cell that utilizes ordered mesoporous metal electrodes. This design requires no carbon, thereby enhancing electrode stability.

Nanoparticle-based mesostructure discovery[1]

Determining how nanoparticle size influences co-assembly with block copolymers is of fundamental and practical importance: understanding this effect can provide guidelines for mesostructure design and can enable mesostructure discovery.

I developed a sol-gel method that produces silica-type nanoparticles of four sizes (Fig. 2A). Each set of nanoparticles was added to a small or large poly(isoprene-*block*-ethyleneoxide) (PI-*b*-PEO) polymer (13 or 28 kg/mol, ~15 wt.% PEO). A lamellar morphology (Fig. 2H) was expected to form based on the polymer:nanoparticle ratio.

When the three smallest sets of nanoparticles were added to the small polymer, a lamellar mesostructure formed (Fig. 2B). Surprisingly, when the largest nanoparticles were added to the

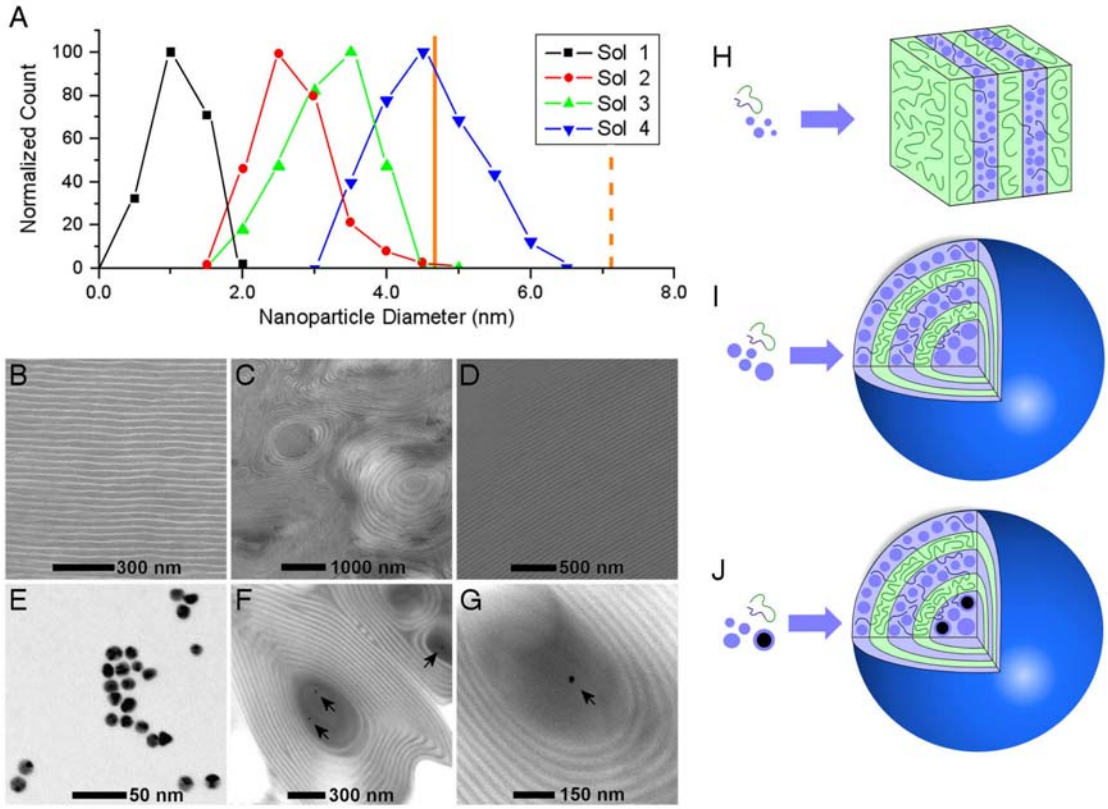

Fig. 2. (A) Size distributions of four nanoparticle syntheses (Sols 1-4), from atomic force microscopy (AFM) height measurements. Orange lines plot the root-mean-square end-to-end distance of the PEO chain (solid=small polymer, dashed=large polymer). **(B)-(G)** Bright field TEM images. **(B)** A lamellar structure produced by mixing Sols 1, 2, or 3 with the small polymer. **(C)** An onion morphology resulting from Sol 4 and the small polymer. **(D)** A lamellar morphology resulting from Sol 4 and the large polymer. **(E)** Gold-silica core-shell nanoparticles. **(F),(G)** Isolation of gold nanoparticles exclusively in onion core. Arrows indicate nanoparticle location. **(H)-(J)**, Illustrations of size-dependent self-assembly. PEO and nanoparticles are blue, PI is green, gold is black.

small polymer, an onion-like structure self-assembled (Fig. 2C). The core of each onion consists of silica nanoparticles; a lamellar structure self-assembles around the core (Fig. 2I). Finally, when the large nanoparticles were added to a large PI-*b*-PEO copolymer, a lamellar morphology formed again (Fig. 2D).

The onion morphology can be understood by considering Fig. 2I. When the nanoparticle diameter approaches the size of the PEO chains, nanoparticle solubility in the PEO decreases. This arises because large nanoparticles occupy an impenetrable region of space, limiting the polymer's conformations. To increase entropy, the largest nanoparticles are expelled from the PEO, resulting in onion mesostructures.

This approach enables the design of compositionally heterogeneous structures by tailoring nanoparticle size distributions to segregate particles into precisely controlled locations (Fig. 2J). As a proof of principle, large gold-silica core-shell nanoparticles (Fig. 2E) were directed exclusively into the onion cores (Fig. 2F,G). These results reveal the power of working with appropriately designed nanoparticle size distributions for controlled nanoparticle placement in segregated mesostructures.

A generalized sol-gel chemistry platform[2]

To increase functionality, it is necessary to move beyond silica. I present a sol-gel chemistry platform (Fig. 3) that incorporates exceptionally high loadings of biological and metallic functionalities.

I found that 3-isocyanatopropyltriethoxysilane (ICPTS) reacts efficiently with amino acids, hydroxy acids, and peptides, forming a ligand that complexes many metals, including Ag, Bi, Co, Cr, Cu, Er, Eu, Gd, In, Mg, Mn, Mo, Pb, Pd, Pt, Rh, Sr, Y, and Zn (Fig. 3A,B). To make sol-gel hybrids, the complex is dissolved in tetrahydrofuran, water is added, and a film is cast. Fig. 3C shows photographs of typical hybrids; ^{29}Si solid state NMR confirms Si-O-Si bonding. This process is compatible with templating (Fig. 3D) and block copolymer co-assembly (Fig. 3E).

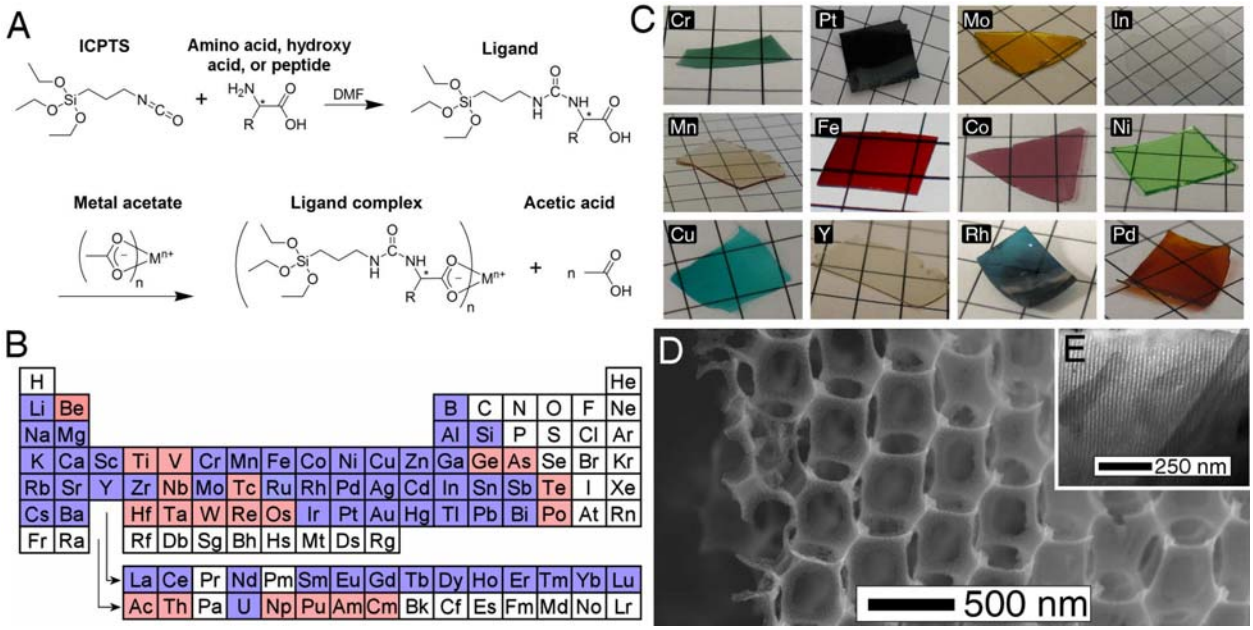

Fig. 3. (A) Synthesis of the ligand complex. **(B)** Metals that can potentially be incorporated. Blue shows commercially available metal acetates, red shows metal acetates that have been synthesized but are not commercially available. **(C)** Photographs of sol-gel hybrids. Grid paper has 5 mm markings. **(D)** Scanning electron microscope (SEM) image of a pyrolized material templated by a polystyrene colloidal crystal. **(E)** TEM image of a sol-gel-block copolymer hybrid supported on holey carbon, which is the source of contrast in the lower right corner.

The hybrids can be used to make a wealth of mesoporous nanocomposites. For example, calcination of a Pd-based hybrid (Fig. 3C) in air and reduction in hydrogen leads to highly dispersed Pd nanoparticles in mesoporous silica (Fig. 4A). Higher Pd loadings are achieved by mixing in additional Pd salts during hybrid synthesis. Pyrolysis produces mesoporous Pd-carbon-silica composites with Pd percolation networks (Fig. 4B). HF etching and/or calcination converts Pd-carbon-silica composites into Pd-carbon (Fig. 4C), Pd-silica, and Pd-only mesostructures (Fig. 4D). A cross-sectional energy dispersive spectroscopy (EDS) analysis (Fig. 4E) suggests macroscopic homogeneity.

One of the most exceptional properties of the nanocomposites is their electrical conductivity. A report in Nature[3] described mesoporous sol-gel nanocomposites with an electrical conductivity of ~0.0005 S/cm, the highest reported. The mesoporous Pd-silica-carbon nanocomposites have conductivities up to 20 S/cm (Fig. 4F), more than 4 orders of magnitude improvement. Importantly, this conductivity is high enough to efficiently carry the current

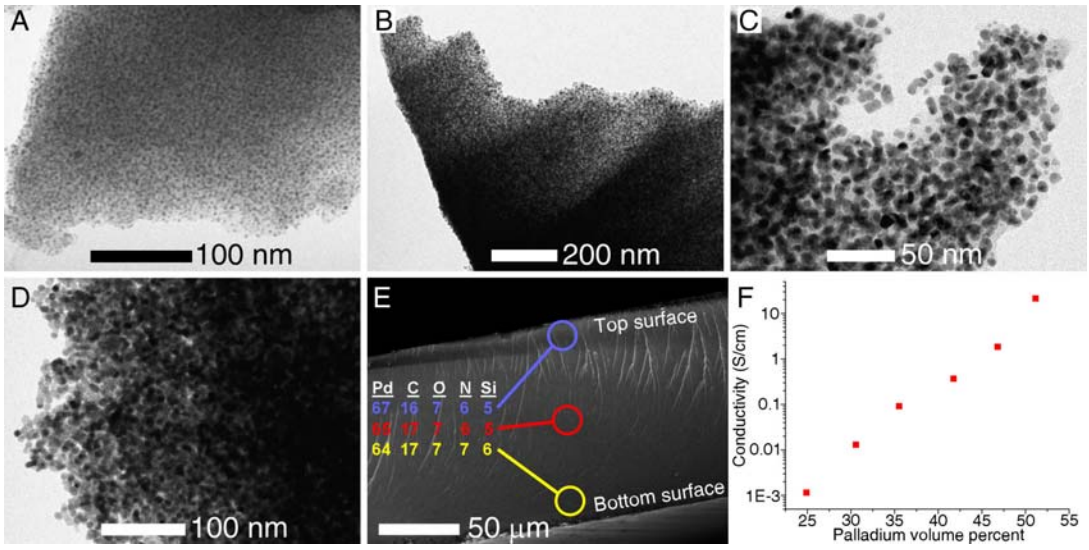

Fig. 4. (A)-(D) Representative bright field TEM images of mesoporous Pd composites. **(A)** Pd-SiO_2 nanocomposite with 10 vol.% Pd. **(B)** Pd-carbon-SiO_2 nanocompsite with 42 vol.% Pd. **(C)** Pd-carbon nanocomposite. **(D)** Mesoporous Pd after removal of silica and carbon. **(E)** Cross section of a pyrolized composite in SEM with EDS performed at the top, middle, and bottom of the film. Values are in wt.%. **(F)** Electrical conductivity as a function of Pd vol.%.

densities achieved in fuel cell electrodes, assuming typical geometries. The ability to extend this approach to other metals, incorporate biological functionality, and utilize templating and co-assembly with block copolymers opens a diverse area for future explorations.

Metal nanoparticles with liquid behavior[4]

To self-assemble ordered mesoporous metals from block copolymers (Fig. 1B), I began exploring metal nanoparticles. Despite potential advantages of mesoporous metals, they have not been produced from nanoparticle-block copolymer self-assembly. This is primarily because metal nanoparticles have low solubility, typically from 1 to 10 mg/mL. To make hybrids with high nanoparticle loadings, solubility should be over 100 mg/mL to allow complete mixing with the block copolymer.

I sought a ligand-mediated route to improve solubility. After exploring many designs, I found that solubility could be enhanced by binding a thiol-containing ionic liquid to the nanoparticle (Fig. 5A, bromide anion). Characterization of the nanoparticles by TEM (Fig. 5B, platinum; 5D, gold) demonstrated that well-defined particles had formed. To further increase solubility, I exchanged the bromide anion for a sulfonate-based anion (Fig. 5A), which led to

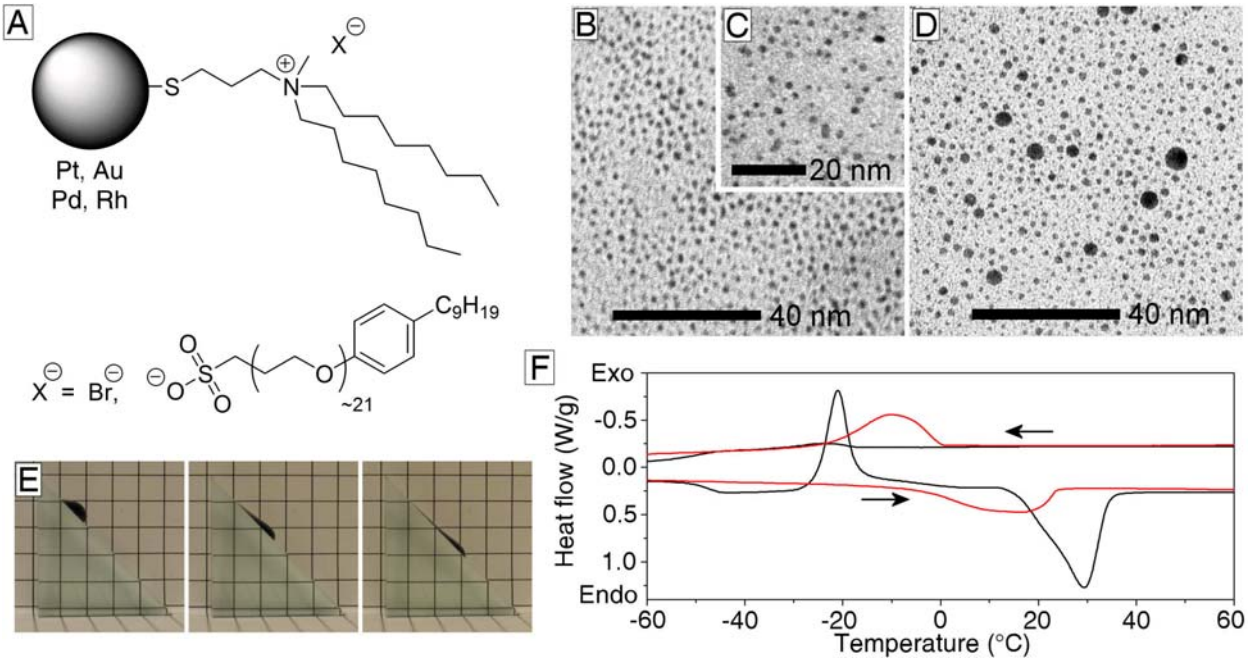

Fig. 5. (A) Design of ligand and nanoparticles (Pt, Au, Pd, Rh). TEM images of platinum particles with bromide anion **(B)** and sulfonate anion **(C)** and gold particles with bromide anion **(D)**. **(E)** Photographs of nanoparticles flowing down a glass slope after 0, 2, and 8 minutes. Grid paper has 5 mm markings. **(F)** DSC traces of the potassium salt of the sulfonate anion (black) and platinum nanoparticles with the sulfonate anion (red).

metal nanoparticles (Fig. 5C, platinum) that were miscible with hydrophobic solvents. In the absence of a solvent, nanoparticles flowed as a liquid (Fig. 5E). Differential scanning calorimetry (DSC, Fig. 5F) confirmed that the nanoparticles melted below room temperature.

This discovery is notable because, until now, most metals had to be heated above 1000 °C to flow as a liquid. These nanoparticles may find use as heat-transfer fluids since the dynamics of nanoparticle flow improve thermal conductivity and the fully accessible phonon modes of metals increase the liquid's heat capacity.

Ordered mesoporous platinum from nanoparticle-block copolymer self-assembly[5]

With an improved understanding of nanoparticle solubility, I developed the first synthesis of ordered mesoporous metals using nanoparticle-block copolymer co-assembly (Fig. 6). It was necessary to re-design the ligand to increase hydrophilicity (Fig. 6A,B). These nanoparticles mix exclusively with the hydrophilic block of the block copolymer, poly(isoprene-*block*-

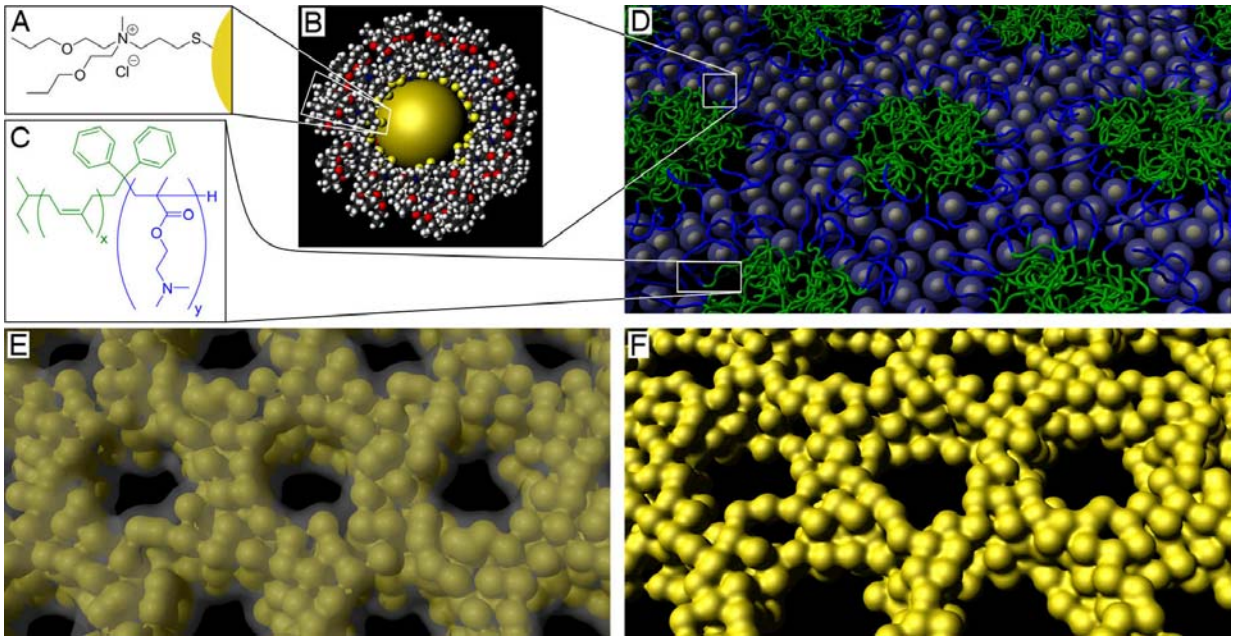

Fig. 6. Ligand **(A)** and nanoparticles **(B)** are co-assembled with PI-*b*-PDMAEMA **(C)** to produce an ordered, mesostructured metal nanoparticle-block copolymer hybrid **(D)**. Pyrolysis of the hybrid yields an ordered mesoporous metal-carbon composite **(E)** and oxidation of carbon yields an ordered mesoporous metal **(F)**.

dimethylaminoethyl methacrylate), PI-*b*-PDMAEMA (Fig. 6C). Dissolution of PI-*b*-PDMAEMA and aged nanoparticles in a methanol-chloroform solution followed by solvent evaporation and annealing afforded inverse hexagonal mesostructures (Fig. 6D, 7A,B). Examining the mesostructure at higher magnification (Fig. 7B) revealed individual platinum nanoparticles within the mesostructure's walls.

To remove organics, the hybrid was pyrolized under nitrogen, yielding a mesoporous platinum-carbon nanocomposite (Fig. 6E, 7C,D). TEM showed that order was retained and that the walls were composed of carbon and crystalline platinum. Physisorption revealed a 17 nm average pore diameter, consistent with TEM measurements. If heated in air instead of nitrogen, carbon was removed but the mesostructure collapsed. This suggests that carbon is needed to maintain order, consistent with a recent report.[6] The mesoporous platinum-carbon nanocomposites have remarkable electrical conductivity. We measured a conductivity of 400 S/cm, the highest value yet reported for mesoporous block-copolymer-derived materials.

An argon-oxygen plasma or nitric-sulfuric acid etch removed carbon at low temperatures. TEM reveals that order is retained and that the carbon is absent (Fig. 6F, 7E). Raman

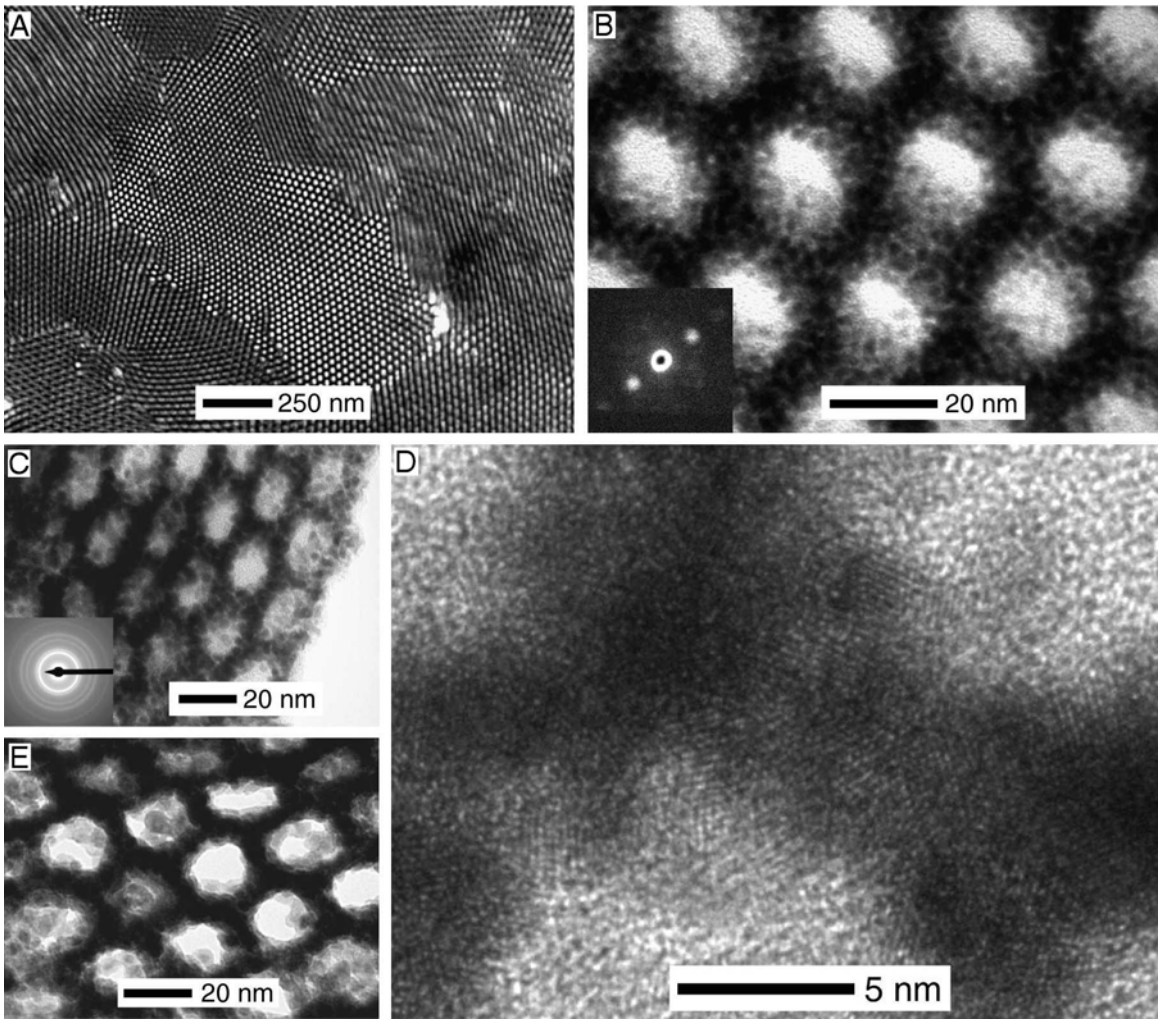

Fig. 7. Bright field TEM images. **(A)** Low magnification view of an inverse hexagonal hybrid. **(B)** High magnification view of the same hybrid. Inset: single-particle electron diffraction. **(C)** An ordered mesoporous platinum-carbon nanocomposite made by pyrolysis of the hybrid. Inset: electron diffraction. **(D)** HRTEM of the same nanocomposite showing Pt lattice fringes. **(E)** Ordered mesoporous platinum.

spectroscopy and EDS confirm carbon removal.

It may be possible to extend this process to other elements, alloys, or intermetallics. Such ordered mesoporous metals may have a range of exceptional electrical, optical, and catalytic properties. Thus, these materials represent the beginning of a new generation of fuel cell electrodes (Fig. 1B).

References

1. Warren, S. C., DiSalvo, F. J., & Wiesner, U. Nanoparticle-tuned assembly and disassembly of mesostructured silica hybrids. *Nature Materials* **6**, 156-161 (2007). Featured in News & Views, Balazs, A., "Economy at the Nanoscale," *Nature Materials* **6**, 94-95 (2007).

2. Warren, S. C., Sai, H., Perkins, M. R., Adams, A. M., Burns, A. A., DiSalvo, F. J. Wiesner, U. Generalized route to highly conductive mesoporous sol-gel materials. *In preparation*. Patent pending.

3. Ryan, J. V., Berry, A. D., Anderson, M. L., Long, J. W., Stroud, R. M., Cepak, V. M., Browning, V. M., Rolison, D. R., Merzbacher, C. I. Electronic connection to the interior of a mesoporous insulator with nanowires of crystalline RuO_2. *Nature* **406**, 169-172 (2000).

4. Warren, S. C., Banholzer, M. J., Slaughter, L. S., Giannelis, E. P., DiSalvo, F. J., Wiesner, U. *Journal of the American Chemical Society* **128**, 12074-12075 (2006). Featured as Editor's Choice, "Flowing Precious Metals," *Science*, **313**, 1542 (2006) and *NanoFocus*, MRS Bulletin (2006).

5. Warren, S. C., Messina, L. C., Slaughter, L. S., Kamperman, M., Gruner, S. M., DiSalvo, F. J., Wiesner, U. *Submitted* (2008).

6. Lee, J. Orilall, M. C., Warren, S. C., Kamperman, M., DiSalvo, F. J., Wiesner, U. Direct access to thermally stable and highly crystalline mesoporous transition-metal oxides with uniform pores. *Nature Materials*, Advanced Online Publication (2008). Featured in Nanowerk and PhysOrg.com.